PROCEEDINGS OF SPIE

SPIEDigitalLibrary.org/conference-proceedings-of-spie

Impacts of degradation on annihilation and efficiency roll-off in organic light-emitting devices

John S. Bangsund, Russell J. Holmes

John S. Bangsund, Russell J. Holmes, "Impacts of degradation on annihilation and efficiency roll-off in organic light-emitting devices," Proc. SPIE 11093, Organic and Hybrid Light Emitting Materials and Devices XXIII, 110930L (3 September 2019); doi: 10.1117/12.2528780

SPIE.

Event: SPIE Organic Photonics + Electronics, 2019, San Diego, California, United States

Downloaded From: https://www.spiedigitallibrary.org/conference-proceedings-of-spie on 09 Sep 2019 Terms of Use: https://www.spiedigitallibrary.org/terms-of-use

Impacts of Degradation on Annihilation and Efficiency Roll-Off in Organic Light-Emitting Devices

John S. Bangsund and Russell J. Holmes*
Department of Chemical Engineering and Materials Science, University of Minnesota, Minneapolis, MN USA 55455

ABSTRACT

Efficiency roll-off and intrinsic luminance degradation are two of the primary limitations of organic light-emitting devices (OLEDs). While both phenomena have been studied separately in detail, they are rarely considered together. Previous analyses of OLED degradation have largely neglected changes in efficiency roll-off and bimolecular quenching, and the magnitude of these changes and their impact on device lifetime remains unclear. We present experimental and modeling results to quantify the magnitude of these changes, which we find range from ~2% to above 10% in magnitude and increase in importance at high brightness or in devices with significant exciton-exciton annihilation.

Keywords: OLED, bimolecular quenching, triplet-polaron quenching, operational lifetime, photoluminescence, phosphorescence

1. INTRODUCTION

Organic light-emitting devices (OLEDs) have achieved widespread commercial success in mobile device displays. However, the performance of OLEDs in high brightness applications such as lighting[1,2] is still limited by the processes of reversible efficiency roll-off[3] and irreversible luminance loss due to intrinsic degradation.[4] Both of these phenomena are primarily caused by bimolecular reactions such as exciton-exciton annihilation and exciton-polaron quenching,[5–8] yet the interplay between roll-off and degradation has rarely been considered. In general, changes in bimolecular quenching (BQ) have been neglected in proposed OLED degradation models,[5,9] and no direct experimental work has been reported to justify this assumption. How large these changes may be, or even their sign, remains unclear. For instance, it has been argued that triplet exciton-polaron quenching increases over time due to accumulated trapped charges,[10] whereas we have previously argued that BQ should become less significant over time due to reduced exciton density and exciton lifetime.[11,12]

Understanding and quantifying degradation-induced changes in BQ could be valuable for several reasons. For OLEDs operated at high brightness, the magnitude of BQ is often initially significant, and hence alleviation of these bimolecular reactions during degradation could serve to improve the device lifetime. Additionally, the slope extracted from accelerated aging at high brightness may be sensitive to the evolution of BQ during degradation. More fundamentally, measurements of changes in BQ could provide insight into the properties of quenching defects and help to validate degradation modeling.

We first provide a theoretical treatment of the degradation dependence of BQ, applying an exciton and polaron dynamics model to estimate how the severity of bimolecular quenching should change in degraded OLEDs. Bimolecular quenching is then probed during degradation using lock-in amplifier measurements of photoluminescence as a function of bias. We find that the magnitude of BQ is generally reduced with degradation due to the proportional losses in exciton density and exciton lifetime with decreasing luminance.

The total measured changes in BQ are typically <5% in magnitude over the course of a typical lifetime test, but they become increasingly important in devices operated at high brightness or devices with significant exciton-exciton annihilation. This study improves understanding of how bimolecular quenching changes in degraded devices and demonstrates that changes in BQ and efficiency roll-off should not be neglected in a complete analysis of OLED degradation.

*jsb@umn.edu, rholmes@umn.edu

Organic and Hybrid Light Emitting Materials and Devices XXIII, edited by Chihaya Adachi, Jang-Joo Kim, Franky So, Proc. of SPIE Vol. 11093, 110930L
© 2019 SPIE · CCC code: 0277-786X/19/$21 · doi: 10.1117/12.2528780

Downloaded From: https://www.spiedigitallibrary.org/conference-proceedings-of-spie on 09 Sep 2019
Terms of Use: https://www.spiedigitallibrary.org/terms-of-use

2. THEORY

The processes of efficiency roll-off and luminance loss can both be described as decreases in the external quantum efficiency (η_{EQE}) of an OLED. The EQE can in turn be expressed as the product of component efficiencies representing each step required to convert injected charge carriers to extracted photons: 1) exciton formation from injected charge carriers (η_{EF}), 2) the fraction of excitons which have an allowed radiative transition to the ground state (χ), 3) the fraction of excitons which relax *via* natural decay (η_τ), as opposed to bimolecular quenching, 4) the fraction of remaining excitons which decay radiatively, i.e. the photoluminescence (PL) efficiency (η_{PL}), and 5) the fraction of emitted photons which escape to the forward-viewing direction, i.e. the outcoupling efficiency (η_{OC}):[12]

$$\eta_{EQE} = \eta_{EF}\chi\eta_\tau\eta_{PL}\eta_{OC} \tag{1}$$

In other formalisms, reductions in η_{EQE} due to bimolecular quenching are described as changes in η_{PL}.[13] Here, we opt to describe these changes with the separate term, η_τ, to distinguish reversible efficiency reductions due to bimolecular quenching from irreversible reductions due to the introduction of exciton quenchers during degradation. Efficiency roll-off at high current densities is typically dominated by changes in η_τ,[3,8] though in some cases changes in η_{EF} or η_{OC} can also contribute.[14,15] Intrinsic luminance loss is typically dominated by losses in η_{EF} and η_{PL}.[11,16,17] As the exciton density and exciton lifetime change with degradation, η_τ is also expected to change.[12] Using a simple model, we will first estimate upper bounds for how much η_τ can be expected to change during degradation.

2.1 Estimating Degradation-Induced Changes in η_τ

To estimate changes in η_τ, we apply a spatially averaged exciton and polaron kinetics model, described previously.[8] While exciton and polaron densities will generally vary spatially, this simple treatment provides a reasonable approximation of how quenching scales with the magnitude of these populations. We treat the case of a phosphorescent emitter and we assume that the dominant excitonic decay processes are 1) natural decay (i.e. the radiative and non-radiative decay of the emitter in the device, defined by lifetime $\tau = 1/(k_r + k_{nr})$), 2) triplet-triplet annihilation (TTA), and 3) triplet-polaron quenching (TPQ). Considering these competing processes, η_τ can be expressed as:

$$\eta_\tau = \frac{n_T/\tau}{n_T/\tau + \frac{1}{2}k_{TT}n_T^2 + k_{TP}n_Tn_P} \tag{2}$$

where n_T is the triplet exciton density, n_P is the polaron density, k_{TT} is the TTA rate constant, and k_{TP} is the TPQ rate constant. Both n_T and n_P will vary with current density (J), whereas τ, k_{TT}, and k_{TP} are assumed to be independent of J. To estimate the impact of degradation on η_τ, we assume that n_P, k_{TT}, and k_{TP} are constant with time. This estimate likely represents an upper bound to the change in η_τ, as charge density typically rises during degradation.[10] Assuming that the radiative rate and η_{OC} are constant, the triplet density will vary proportionally with the normalized electroluminescence intensity (EL):

$$n_T(t) = n_T(0) \times EL(t)/EL(0) \tag{3}$$

The exciton lifetime will vary with time proportionally to the normalized photoluminescence efficiency, (i.e. changes in η_{PL} reflect an increase in the non-radiative decay rate, k_{nr}, and hence decreased τ, as $\eta_{PL} = k_r\tau = k_r/(k_r + k_{nr})$):

$$\tau(t) = \tau(0) \times \eta_{PL}(t)/\eta_{PL}(0) \tag{4}$$

Combining Equations (2)-(4), η_τ can be estimated as a function of EL degradation. For this analysis, we consider changes in η_τ for the archetypical phosphorescent emitter $Ir(ppy)_3$ in a CBP host, taking the measured constants and model from Ref. [8]: $k_{TT} = 7.1 \times 10^{-12}$ cm^3 s^{-1}, $k_{TP} = 0.3 \times 10^{-13}$ cm^3 s^{-1}, $k_F = 1.6 \times 10^{-11}$ cm^3 s^{-1}, $\tau = 6.1 \times 10^{-7}$ s, and a recombination zone width of w = 10 nm. The calculated current density dependence of η_τ, n_T, and n_P for an undegraded device are shown in Figure 1(a). For this device, TTA becomes the dominant exciton decay pathway at high current densities.

In Figure 1(b), the change in η_τ as a function of EL degradation is shown for hypothetical degradation pathways with different degrees of PL degradation. The rise in η_τ is largest when PL degradation is the dominant degradation pathway, almost twice as large as the case where the PL efficiency is constant ($PL/PL_0 = 1$). Physically, these scenarios respectively likely represent degradation dominated by the introduction of exciton quenchers which decrease η_{PL} and degradation *via* the formation of non-radiative charge carrier recombination centers which reduce η_{EF}.[5] When PL

Downloaded From: https://www.spiedigitallibrary.org/conference-proceedings-of-spie on 09 Sep 2019
Terms of Use: https://www.spiedigitallibrary.org/terms-of-use

degradation is dominant, the exciton lifetime is significantly decreased, thus funneling the majority of excitons to natural decay and reducing the magnitude of TTA and TPQ. In practice, most devices show evidence of both degradation pathways,[18] and hence the case where PL loss comprises roughly half of the total degradation ($PL/PL_0 = \sqrt{EL/EL_0}$) provides the best estimate in the absence of direct measurements of PL degradation.[12]

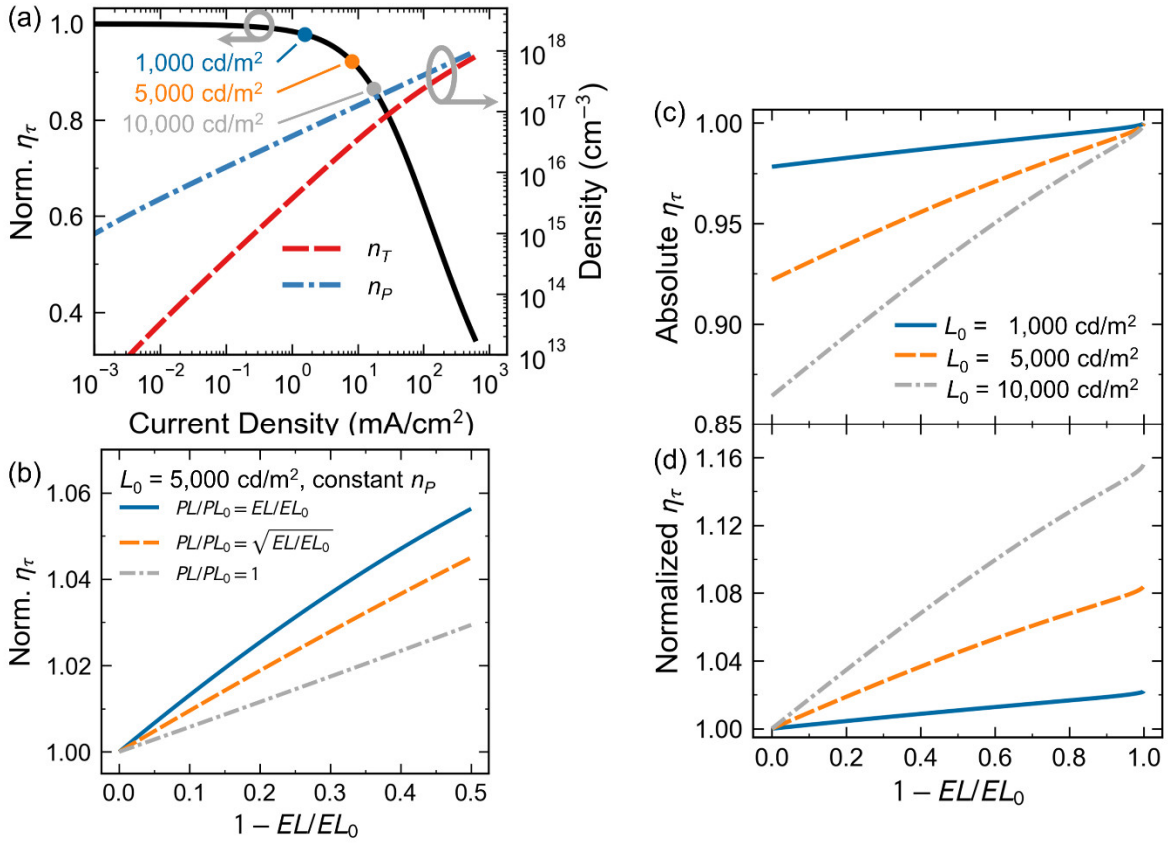

Figure 1. (a) Calculated current density dependence of the natural decay efficiency (η_τ), the triplet exciton density (n_T), and the polaron density (n_P) for an undegraded CBP:Ir(ppy)$_3$ device. (b) Estimated change in η_τ as a function of the degree of EL degradation ($1 - EL/EL_0$). Comparison curves show how the severity of PL degradation impacts η_τ. The rise in η_τ is largest when PL degradation is the dominant degradation pathway ($PL/PL_0 = EL/EL_0$), as the natural lifetime is significantly shortened in this case. These calculations are carried out for a device operated at an initial luminance of L_0 = 5,000 cd/m^2, and polaron density, n_P, is assumed to be constant with degradation. (c) Absolute and (d) normalized change in η_τ as a function of degradation for L_0 = 1,000 cd/m^2, 5,000 cd/m^2, and 10,000 cd/m^2. The rise in η_τ is larger at higher initial luminances, as the initial degree of roll-off is greater. For this calculation, PL degradation is assumed to contribute to half of the total EL degradation ($PL/PL_0 = \sqrt{EL/EL_0}$), and n_P is again constant.

In Figure 1(c)-(d), the degradation-dependent rise in η_τ is shown for several initial luminances, again assuming constant polaron density and that PL loss contributes to about half of the degradation ($PL/PL_0 = \sqrt{EL/EL_0}$). Due to the increasing severity of TTA and TPQ, the rise in η_τ increases in magnitude at higher initial luminance, reaching 10% by EL/EL_0=50% for L_0 = 10,000 cd/m^2. η_τ approaches unity in the limit of complete degradation and the relative rise in η_τ increases at higher luminances due to the lower initial value of η_τ (more severe initial roll-off).

2.2 Influence of Dominant Bimolecular Annihilation Mechanism

We next consider how the exciton quenching kinetics influence the degradation-dependent behavior of η_τ. In Figure 2, we compare two hypothetical devices which have efficiency roll-off dominated by TTA and TPQ, respectively. The TTA dominated device is modeled with the same kinetic parameters as in Figure 1, and the TPQ dominated device is modeled with $k_{TT} = 3.1 \times 10^{-13}$ cm^3 s^{-1} and $k_{TP} = 2.0 \times 10^{-12}$ cm^3 s^{-1} (all other constants are identical). The current-density-dependent roll-off in η_τ, shown in Figure 2(a), display the typical functional dependences for each mechanism. For the

Downloaded From: https://www.spiedigitallibrary.org/conference-proceedings-of-spie on 09 Sep 2019
Terms of Use: https://www.spiedigitallibrary.org/terms-of-use

sake of comparison, we calculate η_τ as a function of degradation for the operating condition at which the roll-off is equivalent for the two devices ($J = 47$ mA/cm^2), shown in Figure 2(b). In the limit of complete degradation, the η_τ of both devices converges to unity ($\eta_\tau/\eta_{\tau,0} = 1.34$), but at moderate degradation ($1 - EL/EL_0 < 0.5$) the TTA dominated device shows over twice the rise in η_τ as the TPQ dominated device.

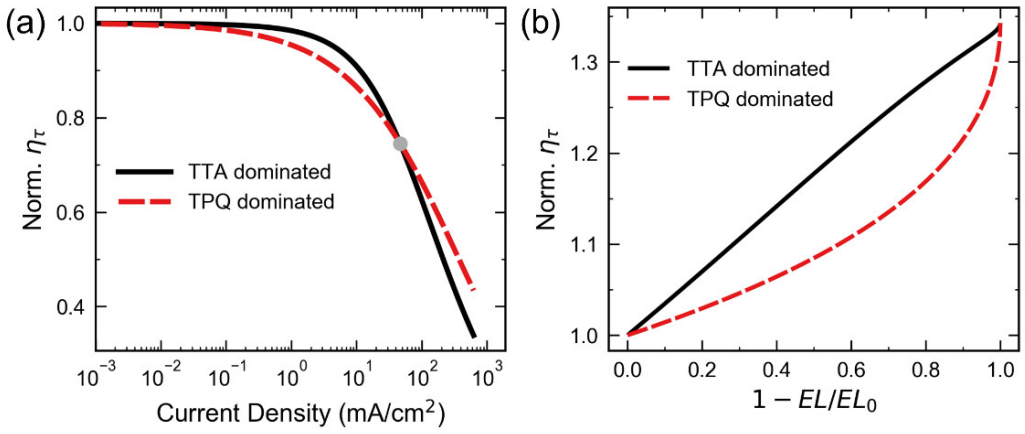

Figure 2. Calculated influence of dominant bimolecular quenching mechanism on degradation-induced changes in η_τ. (a) Current density dependence of η_τ for a hypothetical TTA dominated device ($k_{TT} = 7.1 \times 10^{-12}$ cm^3 s^{-1} and $k_{TP} = 3.3 \times 10^{-13}$ cm^3 s^{-1}) and a hypothetical TPQ dominated device ($k_{TT} = 3.1 \times 10^{-13}$ cm^3 s^{-1} and $k_{TP} = 2.0 \times 10^{-12}$ cm^3 s^{-1}). The circle at 47 mA/cm^2 denotes the operating condition at which total roll-off is equal for the two devices. (b) η_τ as a function of EL degradation for the TTA and TPQ dominated devices at the matched operating condition (J = 47 mA/cm^2). PL degradation is again assumed to contribute to half of the total EL degradation ($PL/PL_0 = \sqrt{EL/EL_0}$), and n_P is constant. For both calculations, the initial triplet exciton density is $n_T(0) = 1.3 \times 10^{17}$ cm^{-3} and $n_P = 2.7 \times 10^{17}$ cm^{-3}.

These results indicate that changes in η_τ should effectively serve to improve device stability at high luminance. Further, the active bimolecular quenching mechanism may impact the operational lifetime *via* the degradation behavior of η_τ.

3. RESULTS AND DISCUSSION

With these upper bound estimates now established for degradation-induced changes in η_τ, we will directly measure these changes using a photoluminescence probe of exciton quenching similar to previously reported methods.[19,20]

3.1 Experimental Methods

Devices with an active area of 25 mm^2 were fabricated on glass substrates pre-patterned with a 150-nm-thick anode layer of indium-tin-oxide (ITO, Xinyan). Substrates were cleaned with solvents followed by exposure to ambient UV-ozone. A hole-injection layer of poly(thiophene-3-[2[(2-methoxyethoxy)ethoxy]-2,5-diyl) (AQ1250, Sigma Aldrich) was spin-cast on the ITO anode in a N_2 glovebox and annealed for 30 minutes at 150 °C. The remaining layers are deposited by vacuum thermal evaporation at a base pressure <7×10^{-7} Torr and a rate of 0.3 nm/s. Devices are encapsulated with epoxy and a cover glass in a N_2 glovebox. Thermally evaporated organic materials were purchased from Lumtec (sublimed grade) and used as received: 4,4',4"-tris(N-carbazolyl)triphenylamine (TCTA), 4,4'-Bis(N-carbazolyl)-1,1'-biphenyl (CBP), fac-tris(2-phenylpyridine)iridium(III) (Ir(ppy)$_3$), and tris-(1-phenyl-1H-benzimidazole) (TPBi).

An Agilent 4155C parameter analyzer and a large area photodiode (Hamamatsu S3584–08) were used to measure device current and luminance as a function of bias, and Lambertian emission was assumed for luminance calculations. A Princeton Instruments FERGIE integrated spectrograph was used to collect electroluminescence (EL) spectra.

A Keithley 2636B was used to source a constant device current and to measure device EL during device lifetimes tests. Every 5% of luminance degradation, the lifetime test was paused and measurements of EQE and PL were taken with voltage sweeps ranging from 0 V to the last operating voltage (measured while current is applied to the device immediately before pausing the lifetime test). Devices were optically pumped with a 100 mW λ=405 nm laser (Coherent OBIS 405LX), which was chopped at nominally 2 kHz, attenuated with a neutral density filter, and expanded with a Thorlabs GBE05-A 5X achromatic Galilean beam expander to a 1/e^2 diameter of ~4 mm. Beam expansion serves to improve signal without increasing the exciton density. Devices were masked to prevent excitation outside the device area. The PL signal was

Downloaded From: https://www.spiedigitallibrary.org/conference-proceedings-of-spie on 09 Sep 2019
Terms of Use: https://www.spiedigitallibrary.org/terms-of-use

passed through a 450 nm long pass filter to prevent detection of stray laser light, collected with a Thorlabs PDA36A Si adjustable gain photodetector, and measured with a Stanford Research Systems SR810 lock-in amplifier. The lock-in amplifier serves to reject the baseline EL signal, ensuring only PL is measured. The PL signal was kept below an equivalent brightness of 50 cd/m^2, ensuring that the probe has minimal impact on quenching. A schematic of the measurement set-up is shown in Figure 3(a).

3.2 Measuring Degradation-Induced Changes in η_τ

The OLEDs of interest are based on the archetypical phosphorescent emitter Ir(ppy)$_3$ doped in a CBP host. The device architecture, shown in Figure 3(b), includes a TCTA hole transport layer (HTL) and a TPBi electron transport layer (ETL). While these transport layers differ from those employed previously,[8] the EQE roll-off shown in Figure 3(c) is almost identical to the previous report. Above J = 1 mA/cm^2, the lock-in measurement of PL shows a similar degree of roll-off as the EQE, confirming that EQE roll-off is dominated by bimolecular quenching and hence reductions in η_τ. The slight discrepancy between lock-in PL and EQE roll-off likely reflects the current-density dependence of charge leakage and exciton formation efficiency. It is also possible the recombination zone (i.e. the spatial profile of electrically generated excitons) differs from the optically generated exciton profile, causing the measurement to slightly underestimate the total degree of exciton quenching. We minimize this spatial mismatch effect by employing thin emissive layers (10 – 20 nm).[11]

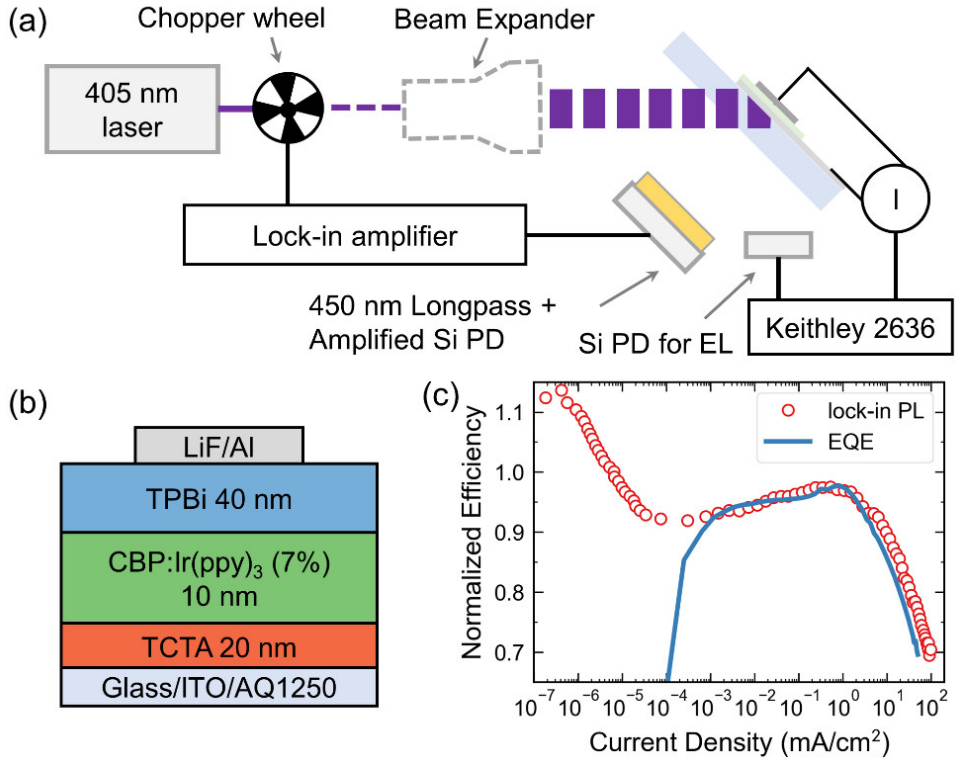

Figure 3. (a) Schematic of experimental set-up. (b) Device architecture for the archetypical CBP:Ir(ppy)$_3$ device studied here. (c) Comparison of lock-in PL measurement (symbol) as a function of applied current density with EQE (blue solid line). At current densities above J = 1 mA/cm^2, the roll-off in lock-in PL is almost identical to the roll-off in EQE, confirming that reductions in η_τ dominate the EQE roll-off. The ~20% drop in lock-in PL at low current densities is attributed to TPQ with injected holes prior to turn-on.

Below turn-on (<2.5 V, $J < 10^{-5}$ mA/cm^2), a drop in PL of ~20% is observed. This low current PL quenching does not appear to be a measurement artifact, as it is observed across a range of laser fluences, chopping frequencies, pump wavelengths. We have also observed this effect to varying extents in other device architectures and materials systems. This result is somewhat surprising, as conventionally quenching is thought to be significant only at current densities above ~1 mA/cm^2.[3] Yet, a previous report showed a ~5% decline in PL lifetime below 1 mA/cm^2,[13] and recent modeling work on a CBP:Ir(ppy)$_3$-based device suggested that TPQ was the dominant deactivation pathway at low biases.[15]

Downloaded From: https://www.spiedigitallibrary.org/conference-proceedings-of-spie on 09 Sep 2019
Terms of Use: https://www.spiedigitallibrary.org/terms-of-use

Based on these previous reports, the low current drop in PL likely arises from TPQ with holes which accumulate prior to turn-on, while the subsequent rise in PL between 3 V and 4.5 V reflects the reduction of hole density above turn-on due to recombination with injected electrons.[15] This behavior cannot be described by the simplified polaron dynamics in the spatially averaged model considered in Section 2. The apparent polaron density needed to describe this behavior is shown in Figure 4, showing significant accumulation at much lower biases than predicted by the simplified model. This full dependence could be more rigorously treated with a drift-diffusion formalism, and the large n_P at low biases is probably partly due to the permanent dipole moment of TPBi.[10,21] However, describing the full bias-dependence is beyond the scope of this work. We are instead interested in understanding the degradation-dependent behavior of η_τ at a fixed current density – as is relevant to a typical lifetime test.

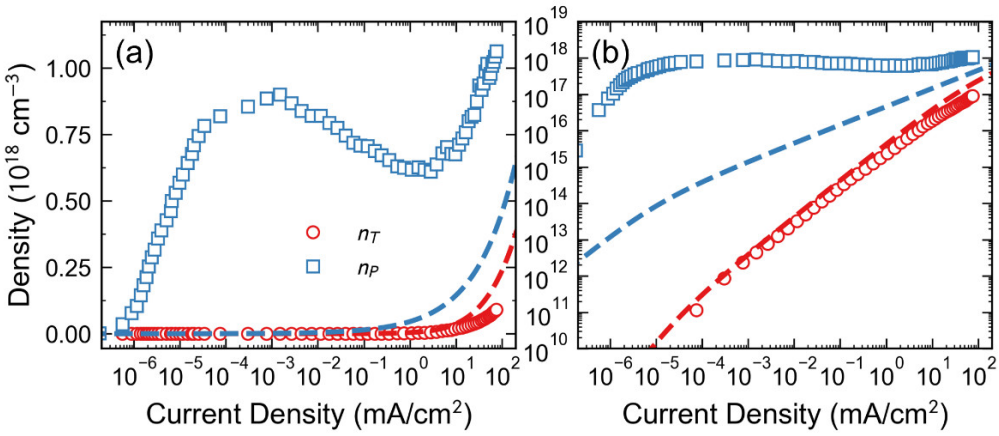

Figure 4. Apparent densities of triplet excitons (n_T) and polarons (n_P) as a function of current density for the CBP:Ir(ppy)$_3$ device. Data in (a) and (b) are identical but plotted on linear-logarithmic and logarithmic-logarithmic scales for clarity. n_T is extracted from luminance measurements by assuming a recombination zone width of w = 10 nm, outcoupling efficiency of η_{OC} = 0.21, and exciton lifetime of τ = 0.69 µs. n_P is extracted from the lock-in PL data from Figure 3 using Eqn. (2) and fixed quenching parameters: $k_{TT} = 8.5 \times 10^{-12}$ cm^3 s^{-1}, and $k_{TP} = 4.0 \times 10^{-13}$ cm^3 s^{-1} (similar to those found in Ref [8]). Dashed lines are calculated using the spatially averaged dynamics model.[8] The slight deviation between extracted and calculated n_T likely reflects current-dependent charge leakage. The large deviation between extracted and calculated n_P is due to simplicity of the polaron dynamics model, which does not account for injection barriers or field-dependent mobility.

Figure 5 shows the degradation dependence of PL and η_τ for devices operated at L_0 = 5,000 and 10,000 cd/m^2. PL measurements are taken intermittently during the lifetime test with and without an applied current. As shown in Figure 5(b), PL measured with an applied J decays more slowly than PL with J = 0. This slower decay corresponds to a reduction in bimolecular quenching and a rise in η_τ, as shown in Figure 5(c). Similar to the trends predicted in Figure 1(c), the rise in η_τ increases at higher luminances, ranging from 7.3% at EL/EL_0=50% for L_0 = 5,000 cd/m^2 to 11.2% by EL/EL_0=50% for L_0 = 10,000 cd/m^2. These increases in η_τ are significant and further indicate that changes in η_τ should not be neglected in a quantitative analysis of OLED degradation at high operating luminances.

Shown in Figure 5(c) as dashed lines are fits based on Equations (2)-(4), where polaron density is assumed to be constant with degradation, exciton density is calculated as described in the caption of Figure 4, the exciton lifetime is fixed at τ = 0.69 µs, and k_{TP} is fixed at 4.0×10^{-13} cm^{-3}. k_{TT} is varied to simultaneously fit the two lifetime tests and n_P is allowed to vary between tests, resulting in the extracted parameters $k_{TT} = 8.5 \times 10^{-12}$ cm^3 s^{-1} and $n_P = 4.8 \times 10^{17}$ cm^{-3} for L_0 = 5,000 cd/m^2 and $n_P = 4.4 \times 10^{17}$ cm^{-3} for L_0 = 10,000 cd/m^2. These parameters agree well with previous reports for similar devices,[7,8] and while the extracted polaron densities are larger than calculated by these previous models, they are in line with expectations from drift-diffusion calculations.[15] The divergence between the fit and the data at high degradation (EL/EL_0<50%) could indicate that the constant polaron density approximation is no longer valid, as accumulated trapped charges may contribute to TPQ and offset the expected rises in η_τ.

This agreement suggests that the assumption of constant n_P provides a reasonable approximation to changes in η_τ. Alternative explanations invoking a non-constant polaron density cannot be entirely ruled out, however. The accuracy of predictions made with the constant n_P assumption is inherently limited by knowledge of the inputs of polaron density and kinetic parameters. If the input k_{TT} and k_{TP} are inaccurate, the degradation data could only be explained by non-negligible changes in polaron density.

Downloaded From: https://www.spiedigitallibrary.org/conference-proceedings-of-spie on 09 Sep 2019
Terms of Use: https://www.spiedigitallibrary.org/terms-of-use

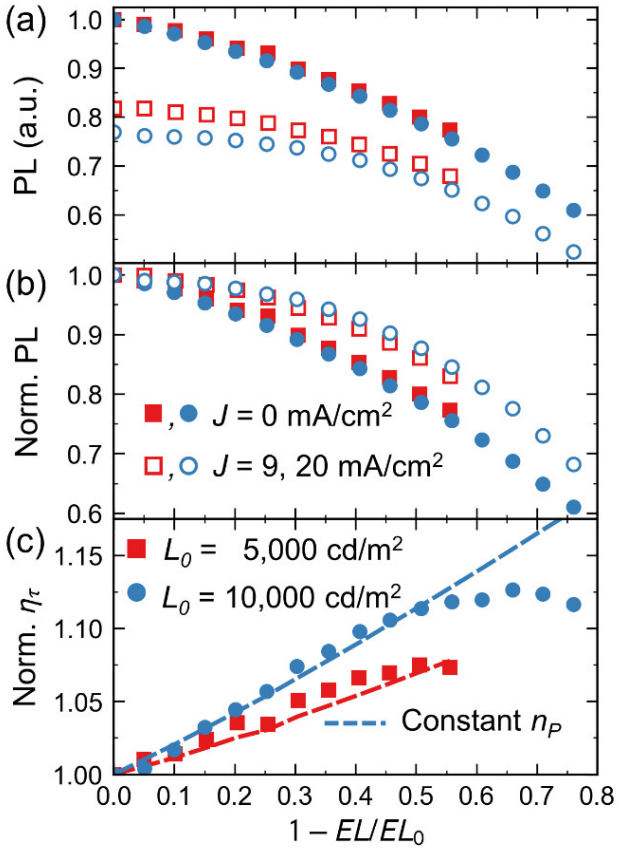

Figure 5. (a) Absolute PL decays for a CBP:Ir(ppy)$_3$ device operated at L_0 = 5,000 and 10,000 cd/m^2. Solid symbols are PL measured with the current off (J = 0 mA/cm^2) and open symbols are PL measured with the current on (J = 9 and 20 mA/cm^2). The lower PL with the current on reflects bimolecular quenching. For undegraded devices, $\eta_\tau = 0.82$ at 5,000 cd/m^2 and $\eta_\tau = 0.77$ at 10,000 cd/m^2. (b) Normalized PL decays from (a). PL with the current on decays more slowly than PL with the current off, indicating a reduction in bimolecular quenching (i.e. a rise in η_τ). (c) Normalized η_τ measured from lock-in PL ($\eta_\tau = PL(J_{op}, t)/PL(J_{norm} = 0, t)$). Lines are fits based on Eqn. (2)-(4) and an assumption of constant polaron density.

To illustrate this, we calculated the expected rise in η_τ for devices with quenching dominated by TTA, dominated by TPQ, or by some combination of the two (Figure 6(a)). The device with equal contributions of TTA and TPQ shows the best agreement with the data. The device dominated by TTA exceeds the data, indicating that polaron density would need to rise during degradation and TPQ would need to increase in magnitude to describe the data. However, the case of dominant TTA is unlikely, as the quenching below 3 V can only be explained by polaron quenching or field quenching. It is instead more likely that TTA and TPQ contribute comparably to overall quenching, or that TPQ is dominant.[13] For devices with more dominant TPQ, the constant n_P assumption underestimates the rise in η_τ, implying that polaron density would need to decline to match the measured rise. While defect quenching models predict that the *free* polaron density will decline during degradation,[5,9] the total charge density generally rises due to the accumulation of trapped charge.[10,18] Whether these trapped charges can quench excitons has not been directly demonstrated, but it seems unlikely that the reductions in free polaron density would be sufficient to explain this discrepancy.

The change in polaron density needed to match the data for each of these scenarios is shown in Figure 6(b). For the case of equal contributions of TTA and TPQ, polaron density stays roughly constant until EL/EL$_0$ = 50%. At higher levels of degradation, polaron density then begins to rise. Regardless of the TTA:TPQ ratio, a rise in polaron density is always needed to describe the data at high degradation. This most likely occurs due to either a reduction in emissive layer mobility[10] or due to trapped charges.[18]

Downloaded From: https://www.spiedigitallibrary.org/conference-proceedings-of-spie on 09 Sep 2019
Terms of Use: https://www.spiedigitallibrary.org/terms-of-use

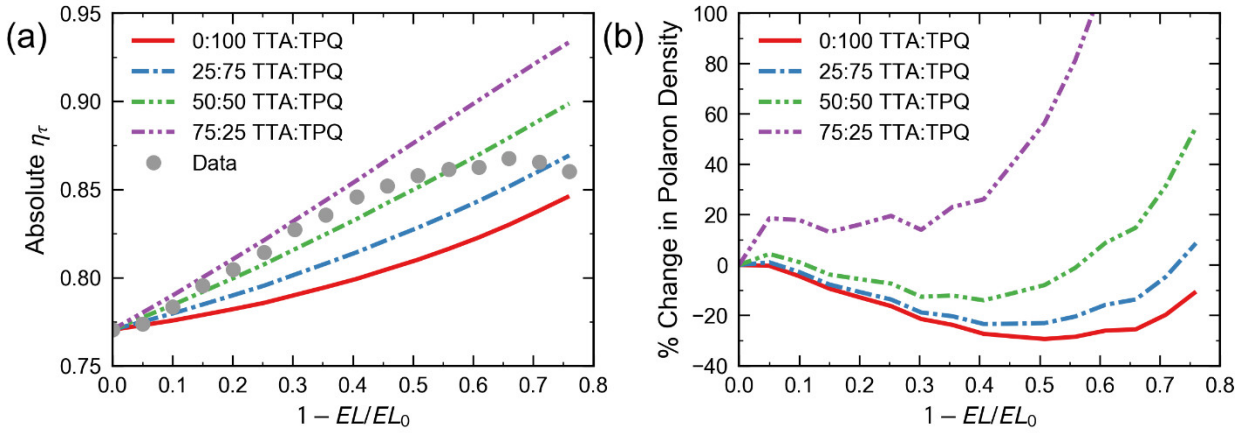

Figure 6. (a) η_τ as a function of EL degradation measured from lock-in PL ($\eta_\tau = PL(J_{op}, t)/PL(J_{norm} = 0, t)$) for an initial luminance of 10,000 cd/m^2. Lines are estimates based on Eqn. (2) and an assumption of constant polaron density. The relative contributions of TTA and TPQ to the overall quenching are varied from 0:100 TTA:TPQ (only TPQ) to 75:25 (predominantly TTA). The k_{TT} used in these calculations is 0 cm^3 s^{-1}, 3.25×10^{-12} cm^3 s^{-1}, 7.15×10^{-12} cm^3 s^{-1}, and 11.5×10^{-12} cm^3 s^{-1} for 0:100, 25:75, 50:50, and 75:25 TTA:TPQ, respectively. The product $k_{TP}n_P$ is varied in each case to match the initial value of $\eta_\tau = 0.77$. (b) Percent change in polaron density as a function of EL degradation which would be needed to describe the measured η_τ from (a) for different initial contributions of TTA and TPQ.

4. CONCLUSIONS

We have presented an analysis of the degradation-induced changes in bimolecular quenching and efficiency roll-off in an archetypical phosphorescent OLED. Using lock-in amplifier measurements of photoluminescence, bimolecular quenching can be directly characterized during degradation of OLEDs. We find that the natural decay efficiency (η_τ) typically rises by less than 5% (reflecting reduced bimolecular quenching) but becomes increasingly important at high luminance, at times exceeding 10%. The magnitude of these changes quenching can be estimated by accounting for the reductions in exciton density and exciton lifetime during degradation and assuming polaron density remains constant. However, at high levels of degradation ($EL/EL_0 < 50\%$), reduced roll-off is partly offset by increased polaron density due to either trapped charges or reduced mobility. This study underscores that the degradation behavior of η_τ should not be neglected when degrading devices at high luminance ($L_0 \geq 5{,}000$ cd/m^2) or in devices with significant exciton-exciton annihilation.

ACKNOWLEDGMENTS

Funding and support for this work was provided by DuPont Electronics and Imaging. The authors acknowledge helpful discussion with Dr. Dominea Rathwell, Dr. Peter Trefonas, Hong-Yeop Na, and Jeong-Hwan Jeon. J.S.B. acknowledges support from the National Science Foundation Graduate Research Fellowship under Grant No 00039202.

Downloaded From: https://www.spiedigitallibrary.org/conference-proceedings-of-spie on 09 Sep 2019
Terms of Use: https://www.spiedigitallibrary.org/terms-of-use

REFERENCES

[1] Reineke, S., Thomschke, M., Lüssem, B. and Leo, K., "White organic light-emitting diodes: Status and perspective," Rev. Mod. Phys. **85**(3), 1245–1293 (2013).

[2] Gather, M. C., Köhnen, A. and Meerholz, K., "White Organic Light-Emitting Diodes," Adv. Mater. **23**(2), 233–248 (2011).

[3] Murawski, C., Leo, K. and Gather, M. C., "Efficiency Roll-Off in Organic Light-Emitting Diodes," Adv. Mater. **25**(47), 6801–6827 (2013).

[4] Scholz, S., Kondakov, D., Lüssem, B. and Leo, K., "Degradation Mechanisms and Reactions in Organic Light-Emitting Devices," Chem. Rev. **115**(16), 8449–8503 (2015).

[5] Giebink, N. C., D'Andrade, B. W., Weaver, M. S., Mackenzie, P. B., Brown, J. J., Thompson, M. E. and Forrest, S. R., "Intrinsic luminance loss in phosphorescent small-molecule organic light emitting devices due to bimolecular annihilation reactions," J. Appl. Phys. **103**(4), 044509 (2008).

[6] Schmidbauer, S., Hohenleutner, A. and König, B., "Chemical Degradation in Organic Light-Emitting Devices: Mechanisms and Implications for the Design of New Materials," Adv. Mater. **25**(15), 2114–2129 (2013).

[7] Reineke, S., Walzer, K. and Leo, K., "Triplet-exciton quenching in organic phosphorescent light-emitting diodes with Ir-based emitters," Phys. Rev. B **75**(12), 125328 (2007).

[8] Hershey, K. W. and Holmes, R. J., "Unified analysis of transient and steady-state electrophosphorescence using exciton and polaron dynamics modeling," J. Appl. Phys. **120**(19), 195501 (2016).

[9] Zhang, Y., Lee, J. and Forrest, S. R., "Tenfold increase in the lifetime of blue phosphorescent organic light-emitting diodes," Nat. Commun. **5**, 5008 (2014).

[10] Schmidt, T. D., Jäger, L., Noguchi, Y., Ishii, H. and Brütting, W., "Analyzing degradation effects of organic light-emitting diodes via transient optical and electrical measurements," J. Appl. Phys. **117**(21), 215502 (2015).

[11] Bangsund, J. S., Hershey, K. W. and Holmes, R. J., "Isolating Degradation Mechanisms in Mixed Emissive Layer Organic Light-Emitting Devices," ACS Appl. Mater. Interfaces **10**(6), 5693–5699 (2018).

[12] Hershey, K. W., Suddard-Bangsund, J., Qian, G. and Holmes, R. J., "Decoupling degradation in exciton formation and recombination during lifetime testing of organic light-emitting devices," Appl. Phys. Lett. **111**(11), 113301 (2017).

[13] Wehrmeister, S., Jäger, L., Wehlus, T., Rausch, A. F., Reusch, T. C. G., Schmidt, T. D. and Brütting, W., "Combined Electrical and Optical Analysis of the Efficiency Roll-Off in Phosphorescent Organic Light-Emitting Diodes," Phys. Rev. Appl. **3**(2), 024008 (2015).

[14] Sim, B., Moon, C.-K., Kim, K.-H. and Kim, J.-J., "Quantitative Analysis of the Efficiency of OLEDs," ACS Appl. Mater. Interfaces **8**(48), 33010–33018 (2016).

[15] Regnat, M., Pernstich, K. P. and Ruhstaller, B., "Influence of the bias-dependent emission zone on exciton quenching and OLED efficiency," Org. Electron. **70**, 219–226 (2019).

[16] Bangsund, J. S., Hershey, K. W., Rathwell, D. C. K., Na, H.-Y., Jeon, J.-H., Trefonas, P. and Holmes, R. J., "Improved stability in organic light-emitting devices by mixing ambipolar and wide energy gap hosts," J. Soc. Inf. Disp. **0**(0), 1–8 (2019).

[17] Winter, S., Reineke, S., Walzer, K. and Leo, K., "Photoluminescence degradation of blue OLED emitters," Proc SPIE **6999**, 69992N (2008).

[18] Kondakov, D. Y., "The Role of Homolytic Reactions in the Instrinsic Degradation of OLEDs.," [Organic Electronics], F. So, Ed., CRC Press, Boca Raton, FL, 211–242 (2010).

[19] Zou, W., Li, R., Zhang, S., Liu, Y., Wang, N., Cao, Y., Miao, Y., Xu, M., Guo, Q., Di, D., Zhang, L., Yi, C., Gao, F., Friend, R. H., Wang, J. and Huang, W., "Minimising efficiency roll-off in high-brightness perovskite light-emitting diodes," Nat. Commun. **9**(1), 608 (2018).

[20] Shirasaki, Y., Supran, G. J., Tisdale, W. A. and Bulović, V., "Origin of Efficiency Roll-Off in Colloidal Quantum-Dot Light-Emitting Diodes," Phys. Rev. Lett. **110**(21), 217403 (2013).

[21] Noguchi, Y., Miyazaki, Y., Tanaka, Y., Sato, N., Nakayama, Y., Schmidt, T. D., Brütting, W. and Ishii, H., "Charge accumulation at organic semiconductor interfaces due to a permanent dipole moment and its orientational order in bilayer devices," J. Appl. Phys. **111**(11), 114508 (2012).

Downloaded From: https://www.spiedigitallibrary.org/conference-proceedings-of-spie on 09 Sep 2019
Terms of Use: https://www.spiedigitallibrary.org/terms-of-use